MiR-144-3p-mediated dysregulation of EIF4G2 contributes to the development of Hepatocellular Carcinoma through ERK pathway

Shuangshuang Li
Zhejiang University
Jiajia Shao
Zhejiang University First Affiliated Hospital State Key Laboratory for Diagnosis and Treatment of Infectious Diseases
Guohua Lou
Zhejiang University First Affiliated Hospital State Key Laboratory for Diagnosis and Treatment of Infectious Diseases
Chao Wu
Zhejiang University First Affiliated Hospital State Key Laboratory for Diagnosis and Treatment of Infectious Diseases
Yanning Liu (liuyanning@zju.edu.cn)
Zhejiang University First Affiliated Hospital State Key Laboratory for Diagnosis and Treatment of Infectious Diseases
MIN ZHENG (minzheng@zju.edu.cn)
Zhejiang University

Research

Keywords: EIF4G2, HCC, miR-144-3p, ERK1/2, prognosis

Posted Date: September 1st, 2020

DOI: https://doi.org/10.21203/rs.3.rs-66225/v1

Version of Record: A version of this preprint was published on February 1st, 2021. See the published version at https://doi.org/10.1186/s13046-021-01853-6.

Abstract

Background

Hepatocellular carcinoma (HCC) is one of the most common cancers with high incidence and mortality. But the underlying mechanisms of HCC still remain unclear. Eukaryotic translation initiation factors (eIFs), showing a large effect on tumor development. In this study, we were aimed to investigate the role of eukaryotic translation initiation factor 4 gamma 2 (EIF4G2) in HCC.

Methods

Western blot (WB) in 30 paired HCC tissues and tissue microarrays (TMAs) by immunohistochemistry (IHC) in 89 paired HCC samples were performed to assess EIF4G2 expression. Clone formation, Real-Time Cell Analysis (RTCA), wounding-healing and transwell assays were adopted to evaluate the role of EIF4G2 on HCC cell proliferation, migration and invasion ability. The function of EIF4G2 on HCC tumor growth was conducted by xenograft nude mouse model in vivo. The regulation of miR-144-3p on EIF4G2 was performed by luciferase reporter assay and WB.

Results

EIF4G2 was obviously upregulated in HCC tissues, and high-expression of EIF4G2 was closely related to HCC prognosis. EIF4G2 silencing could inhibit HCC cells growth and metastasis in vitro, and suppress tumorigenesis in vivo by repressing ERK signaling pathway. The results of luciferase reporter assay, WB and IHC staining verified that EIF4G2 was negatively regulated by miR-144. And re-expression of EIF4G2 could partially reverse the inhibiting effect of miR-144 in HCC.

Conclusion

In summary, our study revealed the role of EIF4G2 in HCC development by activating ERK pathway. We also found that EIF4G2 could be negatively regulated by tumor suppressor miR-144. Our investigations indicated that EIF4G2 might be a promising therapeutic target in HCC.

Background

Liver cancer ranks the sixth in incidence and the fourth mortality rate among all cancers[1]. Although more and more novel therapies for hepatocellular carcinoma (HCC) have been developed, such as transcatheter arterial chemoembolization(TACE) and liver transplantation, the prognosis of HCC is still very poor, especially the outcome of advanced HCC patients[2]. So, it is very urgent to find new and effective clinical targets of HCC.

Nowadays, the role of eukaryotic translation initiation factors (eIFs) in cancer development has attracted considerable attention. Recent studies revealed dysregulation of eIFs played a major role in carcinogenesis by causing aberrant gene expression[3–5]. Here, we investigated the role of eukaryotic translation initiation factor 4 gamma 2 (EIF4G2), a member of eIFs family, which is a translational activator during the conditions of cellular stress[6–8]. Previous studies have implicated that abnormal expression of EIF4G2 played key roles on the progress of many cancers. For example, suppression of EIF4G2 could significantly repress the development of acute myeloid leukemia development[9], diffuse large B cell lymphoma[10] and human osteosarcoma[11]. However, the role of EIF4G2 in HCC has not been reported. The data from the Human Protein Atlas database displays overexpression of EIF4G2 protein level has a poorer prognosis in HCC[12]. While the mRNA level of EIF4G2 has no significant difference in HCC and adjacent non-cancer tissues[13]. Hence, we guess there is a post-transcriptional regulation of EIF4G2.

The post-transcriptional regulation mechanisms of microRNAs (miRNAs) are very prevalent[14]. A lot of miRNAs were found to have a big effect on HCC development. And our previous study discovered that miR-199a improved HCC chemosensitivity by targeting mTOR[15]. Here, we hypothesized whether the role of EIF4G2 in HCC was regulated by miRNAs.

In this study, we found EIF4G2 was a new disadvantageous factor in HCC. Down-regulation of EIF4G2 could inhibit HCC development through suppression the ERK signaling pathway. Mechanistic studies verified that EIF4G2 was negatively regulated by miR-144-3p.

Methods

HCC patients

Thirty paired HCC cancerous tissues and matched para-cancer tissues were collected from the first affiliated hospital of Zhejiang university, who underwent surgery between September 2016 and March 2017. Patients in this study had not been accepted TACE or chemotherapy or any other treatments. The research was allowed by the Medical Ethics Committee of the hospital. All tissues were frozen at -80 °C immediately. All patients' information was list in Table S1.

Cell lines and cell culture

The human HCC cell lines (Huh7, Huh7-Luc□Huh7 cells stably expressing luciferase□, Hep3B) and 293T cells were cultured with Dulbecco's modified Eagle's medium (DMEM; HyCloneTM #AE29431636) and 10% fetal bovine serum (FBS; CORNING #35081006). The cell lines were harvested via trypsinization and washed by phosphate buffered saline. And all cells were incubated in 5% CO_2 at 37 °C. Huh7-Luc cell line was constructed in our lab previous study[16].

Real-Time Cell Analysis (RTCA)

Cell proliferation assays were monitored by the *xCELLigence* Real-Time Cell Analysis S16 instrument and E-Plate 16 (ACEA Biosciences, Inc.) according to the manufacturers' instructions. The electronic impedance of system changed according to cell status, then cell growth was measured by using a parameter termed the cell index (CI). 50 uL complete media was added into the plates and baseline was measured. Then 5×10^3 cells were seeded into every well and grown for about 80 h at 37 °C in 200 uL culture media. The impedance was detected every 15 min during 72 h after seeding. Data were analyzed by xCELLigence software and the cell index normalized to the data recorded at the time of cell treatment.

RT-qPCR

RNA of cells and tissues were extracted by Trizol (Takara #9109) according to the manufactures' protocol. Then reverse transcription (RT) reaction was performed using PrimeScriptTM RT reagent kit with gDNA eraser (Takara #RR047A) according to the protocol. Quantitative real-time polymerase chain reaction (RT-qPCR) was conducted using TB GreenTM Premix Ex TaqTM (Tli RNaseH Plus), (Takara #RR420A). The results were quantified using the $2^{-\Delta\Delta Ct}$ method. In the present study, GAPDH and U6 were used as reference genes to normalize EIF4G2 and miR-144-3p, respectively. The primers of miR-144-3p and U6 were bought from RiboBio Co., Ltd., China. The primer sequences used were listed in table S2.

Matrigel Invasion Assay

Cell invasion ability was assayed by 8mm Corning transwell insert chambers (Corning), which were coated with 50 μL Matrigel® (Corning®) and placed into 24-well plates. Then the 24-well plates were placed for 30 min at 4 °C, and incubated for 1-2 h at 37 °C. 1×10^5 cells per well in 200 uL serum-free culture medium were seeded into chambers after 48 h of transfection, and 600 uL DMEM with 10% FBS was inserted into the lower chamber. After 48 h, invaded cells were fixed with 4% paraformaldehyde (Servicebio #1101) for 30 min and stained with 0.1% crystal violet (Dawen Biotec) for 30 min. After removing cells on the upper surface, the invaded cells were imaged and counted.

Migration Assay

Cell migration ability was performed with wound-healing assays. Hep3B cells (3×10^5) and Huh7 cells (4×10^5) after 48 h of transfection were seeded into 24 well plates. After cells reached complete confluence, linear wounds were made with 200 μL plastic pipette tips. And cells were cultured in DMEM with 1% FBS. Images were captured at 0, 12, 24, 48 h. Three representative visual fields were selected from each dish, and the cells migration distances were measured with microscope.

Colony formation assay

Five hundred cells after transfection were seeded into 6 cm petri dishes with complete media, and grown up to until visible colonies formed about 2 weeks. Cells were fixed with 4% paraformaldehyde for 30 min and then stained with Coomassie Brilliant Blue (FUDE Biological #FD0022) for 30 min. Washing with deionized distilled water, the dishes were air dried at room temperature. Colonies were counted and

photographed with Molecular Imager® Gel Doc™ XR+ imaging system (BIO-RAD). All assays were repeated three times.

Bioinformatics analysis

The relationship of EIF4G2 and HCC prognosis was from the Human Protein Atlas database. And the data of mRNA level of EIF4G2 was from GEPIA database. miRNAs which can modulate EIF4G2 were predicted by the website of TargetScan, miRCODE, and starBase.

Lentivirus transduction

MiR-144 overexpression and ctrl lentivirus were purchased from GeneChem. Cells were seeded into 6-well plates about 40-50% confluence, and adding 10 uL lentivirus per well. 2 ug/mL puromycin (MCE #NSC3056) were added to select infected cells after 48 h transduction. Subsequently, cells were cultured under 1 ug/mL puromycin to keep stably infected.

Si-RNA and vector transfection

Si-RNAs of EIF4G2 and a negative control RNA were purchased from Genepharma. Cells were transfected with 50 nM si-RNA for 48 h at 37 °C using the Lipofectamine® RNAiMAX (Invitrogen #13778-015) based on the manufacturer's protocol. Overexpression vectors of EIF4G2 and miR-144 and corresponding ctrl vectors were designed and synthetized from GeneChem. Transfection of each vector was carried out using Lipofectamine®3000 (Invitrogen #L3000-015). Total RNA and protein were extracted after 48 h transfection. And transfection efficiency was verified by RT-qPCR and Western blot. Sequences of the si-RNAs were listed in table S3.

Luciferase assay

The wild-type (WT) and mutant (MUT) luciferase reporter vectors of EIF4G2 3'-UTR were obtained from GeneChem. $1x10^4$ 293T cells were seeded into 96-well plates, then the WT and MUT reporter vectors and miR-144 overexpression vector were co-transfected with Lipofectamine 3000 into 293T cells. 48 h later, the firefly and Renilla luciferase activities were assessed by GloMax microplate luminometer (Promega, USA) using Dual-Glo® Luciferase Assay System kit (E2920, Promega, USA). Renilla luciferase activities were used to evaluate transfection efficiency

Western Blotting Analysis

Protein of cells and tissues was extracted with RIPA lysis Buffer (Applygen #C1053), and protein concentration was measured with a BCA assay (Thermo Fisher, #23227). Protein was separated by sodium dodecyl sulfate-polyacrylamide gel electrophoresis (GenScript #M00657), then transferred from gel to 0.2 um polyvinyl difluoride membrane and blocked in TBS-T containing 5% bovine serum albumin (Haoke HK5021) or skim milk powder for 2 h. Then, the membrane was incubated with specific primary antibodies at 4 °C for about 14 h and incubated with secondary antibodies for 1 h at room temperature.

The specific primary antibodies used in this paper are as follows: EIF4G2 (1:1000, CST #2182), p-ERK1/2 (1:1000, CST #4370), ERK1/2 (1:1000, CST #4695), GAPDH (1:1000, CST #5174).

Animal studies

BALB/cJGpt-Foxn1nu/Gpt (BALB/c) female mice (4 weeks old, 12-14 g) were purchased from GemPharmatech Co. Ltd (Nanjing, China), and housed in temperature-controlled and pathogen-free rooms. Water and food were provided free. Huh7-Luc cells (1×10^6) that had been transfected with si-EIF4G2, si-NC, miR-144 overexpression and ctrl lentivirus, were injected subcutaneously into back of mice near their hind legs (7 mice each group). And the left area was ctrl treatment, the right area was experimental treatment. Tumor size was measured every 2 days and tumor volume was calculated using this formula: volume= (length × width^2)/2. Mice were sacrificed after about 20 days by cervical dislocation. And the tumors were removed and weighed and photographed. All protocols of animal studies were approved by the Institutional Animal Care and Use Committee of the First Affiliated Hospital of Zhejiang University.

Tissue microarrays and Immunohistochemistry

The HCC tissue microarray chip including total 89 pairs of HCC tumor tissues and matched para-carcinoma tissues were bought from Shanghai Biochip Company Ltd. IHC staining was performed to assess EIF4G2 expression in HCC tissues according to the manufacturer's protocol using anti-EIF4G2 antibody (dilution 1:400, abcam #ab97302). Each HCC-TMA score was analyzed based on the product of staining intensity and the percentage of positively stained cells. In this study, the positive rate is 100%. If a score less than or equal to 1, we categorized it as EIF4G2 low expression group, and if a score greater than 1, we categorized it as EIF4G2 high expression group.

Statistical analysis

Statistical analyses were performed with SPSS 18.0 and GraphPad Prism 8 software. Data were presented as the mean ± standard deviation (SD). In HCC-TMA chip, Chi-square tests were used to analyze the EIF4G2 expression in HCC and matched tissues. The overall survival (OS) and disease-free survival (DFS) were performed using the Kaplan–Meier method with the log-rank test. The correlation between the expression of EIF4G2 and PDL1 was analyzed by the Spearman's rank correlation test. The correlation between the expression of miR-144 and EIF4G2 protein was analyzed by the Pearson's test. The expression of miR-144 and EIF4G2 in 30 paired HCC tissues was performed using paired t test. HRs and 95% confidence intervals (CIs) for clinical correlative factors were investigated using the Cox regression models in univariate and multivariate analysis. Value of $P<0.05$ was considered to be statistically significant.

Results

EIF4G2 is overexpressed in HCC and high EIF4G2 expression indicates poor prognosis of HCC patients

As shown in Figure 1A, the Human Protein Atlas database demonstrated that HCC patients with high level of EIF4G2 had significantly shortened survival. To explore the role of EIF4G2 in HCC, we detected the expression of EIF4G2 on HCC clinical fresh frozen samples. The result of Western blot displayed the level of EIF4G2 was remarkably enhanced in HCC tissues compared with corresponding para-carcinoma tissues (n=30) (Figure 1B and Figure S1A-B). IHC staining was made with HCC-TMA chip including 89 paired HCC samples. Representative IHC staining intensity of EIF4G2 was shown in Figure 1C, and the score was from 0 to 3. Consistently, the staining result also showed higher expression of EIF4G2 in HCC tumor tissues (Figure 1D). Further analysis of associations between EIF4G2 and clinicopathological characteristics revealed how EIF4G2 overexpression affected HCC development. As shown in Table 1, EIF4G2 overexpression was significantly related to cases with a higher T stage (T2/T3, p=0.01), a higher TNM stage (II/III, p=0.01), HCC recurrence (p=0.044) and with PDL1 positive expression (p=0.035). All HCC patients were followed up at least 7 years, compared to those with low EIF4G2 expression, the cases with higher EIF4G2 expression had no significant difference in OS, but showed a shorter DFS (p=0.025) (Figure 1E-F). Besides, EIF4G2 was positively correlated with PDL1 expression (p=0.009) (Figure 1G). Taken together, EIF4G2 might be an unfavorable prognostic marker in HCC.

EIF4G2 facilitates HCC growth and metastasis in vitro through ERK signaling pathway

Next, we studied the EIF4G2 biological functions in HCC cells. Three siRNAs targeting EIF4G2 were used to choose the better two of knockdown-efficiency by Western blot (Figure 2A). Colony formation assays and RTCA were conducted to address the effect of EIF4G2 on HCC cells growth. The number of clones of si-EIF4G2 group was obviously less than the ctrl group (Figure 2B). Besides, the results of RTCA revealed that EIF4G2 knock-down could significantly inhibit cell growth both in two HCC cells (Figure 2C). On the other hand, the scratch experiment demonstrated that scratch width narrowed more obviously in the ctrl group (Figure 2D). Subsequently, the transwell invasion assay was adopted to study cell invasion. The result displayed that the number of invaded cells of si-EIF4G2 group was less than ctrl group (Figure 2E). In general, downregulation of EIF4G2 suppressed HCC cell migration and invasion ability. To further explore the mechanism of EIF4G2 in HCC, the role of EIF4G2 in ERK signaling was investigated. Activation of ERK signaling pathway is closely related to HCC prognosis and development, and is detectable in nearly half of early HCC patients and almost all patients with advanced HCC[17, 18]. The expression levels of total ERK1/2 and p-ERK1/2 were performed by Western blot in two HCC cells. As shown in Figure 2F, no apparent difference was found for the level of ERK1/2, while the p-ERK1/2 expression was significantly reduced in EIF4G2 silencing groups, and overexpression of EIF4G2 improved the level of p-ERK1/2. These results indicated EIF4G2 facilitated HCC progress in vitro by ERK signaling pathway.

EIF4G2 knockdown suppresses tumorigenesis in vivo

Equal numbers of Huh7-Luc cells ($1x10^6$ cells) infected with si-EIF4G2 and NC were subcutaneously injected into back of female nude mice. The left side of mice was the ctrl group and the right side indicated the experimental group (Figure 3A). Tumors volumes of two groups were measured every two

days and the tumor growth curve was drawn. The curves revealed that there was a significant tumor growth inhibition in EIF4G2 silencing group (Figure 3C). The mice were sacrificed after 18 days and the tumor volume and weight of two groups were weighed (Figure 3B-D). Obviously, downregulation of EIF4G2 suppressed tumor growth in vivo. The expression of EIF4G2 was further confirmed by western blot. In addition, the levels of the ERK1/2 and p-ERK1/2 were also detected. The level of p-ERK1/2 was lower in si-EIF4G2 group than that in NC group (Figure 3E-F).

EIF4G2 is negatively regulated by miR-144

Considering the role of miRNAs in cancer development by restraining targeted mRNAs, we used online database websites to predict the possible miRNAs regulating EIF4G2 expression post-transcriptionally. As shown in Figure 4A, miR-144 might bind with 3'-UTR of EIF4G2. Luciferase reporter assay exhibited that overexpression of miR-144 could inhibit EIF4G2-WT luciferase activity but not EIF4G2-MUT (Figure 4B). The protein level of EIF4G2 was remarkably repressed, after transfecting miR-144 overexpression vector to Hep3B and Huh7 cells (Figure 4C). Furthermore, in our 30 paired HCC samples, the expression of miR-144 was significantly lower in HCC tumor tissues compared with matched para-cancer tissues (Figure 4D). Further Pearson correlation analysis demonstrated the miR-144 expression and EIF4G2 protein levels were negatively correlated in 30 paired HCC samples (Figure 4E). All these data certified that EIF4G2 could be negatively regulated by miR-144.

MiR-144 suppresses HCC development in vitro and in vivo

There were some researches about anti-tumor effect of miR-144[19-21]. In our study, we made a series of experiments to explore the effect of miR-144 in HCC. The efficiency of miR-144 overexpression was performed by qRT-PCR (Figure S1C). The colony formation assays validated that Hep3B and Huh7 cells formed fewer colonies in the miR-144 overexpressed group than the ctrl group (Figure 5A). And the results of RTCA displayed overexpression of miR-144 could inhibit HCC cells growth ability (Figure 5B). Besides, the wound healing and transwell assays demonstrated that upregulation of miR-144 suppressed HCC cells ability for migration (Figure 5C) and invasion (Figure 5D-E). In vivo, the equal numbers of Huh7-Luc cells ($1x10^6$ cells) infected with miR-144 overexpressed lentivirus and control lentivirus vectors were subcutaneously injected into female nude mice (Figure S1D). The left flank of mice was control group and the right flank indicated experimental group. Fluorescent photos of nude mice displayed obvious inhibition effect of miR-144 on tumorigenesis (Figure 5F). The tumor sizes were measured every 2 days (Figure 5G-H). The mice were sacrificed after 22 days and the tumors were weighed (Figure 5I). IHC staining results displayed that mice tumor from miR-144 overexpression group was remarkably reduced in EIF4G2 expression compared with the NC group (Figure 5J). These results implied that miR-144 significantly suppressed HCC xenografts in nude mice. In short, our results were consistent with other studies, which miR-144 played an anti-tumor role in HCC.

Functions of EIF4G2 in HCC are regulated by miR-144

Furthermore, we found that the inhibition effect of miR-144 could be partially reversed by EIF4G2 overexpression. Hep3B and Huh7 cells were transfected with miR-NC, miR-144, miR-144&ctrl vector, miR-144&EIF4G2 overexpression vector. As shown in Figure 6A, overexpression of EIF4G2 could reverse ERK pathway inhibited by miR-144. Besides, the scratch experiments and transwell assays demonstrated that miR-144 induced suppression of HCC cells migration and invasion were remarkably reversed by restoration of EIF4G2(Figure 6B-C). The results verified that miR-144 might be the upstream regulation mechanism of EIF4G2, and miR-144 suppressed HCC development by targeting EIF4G2.

Discussion

HCC is a serious health-threatening disease, which has a very poor prognosis due to lacking of more effective prognostic and therapeutic targets[22, 23]. In this study, we first showed the evidence that EIF4G2 was unfavorable prognostic marker in HCC, and suppression of EIF4G2 could inhibit HCC development.

Many researches have suggested that EIF4G2-dependent mRNAs were specifically involved in the pro-oncogenic activities such as cell proliferation, anti-apoptosis, tumor invasion, metastasis and angiogenesis[6, 7, 24–28]. Therefore, EIF4G2 has been found to be associated with tumor development and treatments. Down-regulation of EIF4G2 could induce re-acquirement of chemo-sensitivity to the paclitaxel in ovarin cancer[29] and enhanced cisplatin chemosensitivity of nonsmall cell lung cancer[30]. Here, we first reported that EIF4G2 was abnormally enhanced in HCC tissues and higher EIF4G2 was associated with some clinicopathological characteristics, such as T stage, TNM stage, recurrence, and poorer DFS of HCC patients. The result of OS in our study had no significant difference, this might be because the number of our samples was too small (n = 89) compared with the database (n = 365). Besides, the positive correlation between EIF4G2 and PDL1 expression reflected that they might be jointly involved in the disease progression and immune escape of HCC, which deserved a further study. Moreover, EIF4G2 could strongly promote HCC cells growth and metastasis, and promote HCC xenografts in nude mice. A paper revealed EIF4G2 promoted the translation of mitogen-activated protein kinase kinase kinase 3, and deletion of EIF4G2 resulted in suppression of the Akt and ERK signaling pathway in mouse embryonic stem cells[31]. Consistently, our study demonstrated that EIF4G2 overexpression could activate the ERK pathway, whereas EIF4G2 silencing produced an opposite result.

Analysis of GEPIA data showed that the level of EIF4G2 mRNA was not significantly different between HCC tissues and para-carcinoma tissues (Figure S1E), while the protein level of EIF4G2 had obvious difference. The results reminded us of the regulatory mechanism of miRNAs. miRNAs take part in post-transcriptional regulation by binding to the 3'UTR of targeted mRNAs, then preventing proteins translation. Using some website database containing TargetScan, miRCODE and starbase, we found that miR-144 was likely a new regulator to modulate EIF4G2, for there were several conserved binding sites between them. miR-144, a well-known tumor suppressor, which has been found to be involved in several cancer developments including HCC. A comprehensive opinion of miR-144 in HCC revealed that many genes and signaling pathways were regulated by miR-144, including toll-like receptor pathway, p53

signaling pathway, cell cycle associated proteins[32]. In addition, miR-144 could inhibit human hepatocellular carcinoma by regulating CCNB1[33], repress mTOR-VEGF pathway by targeting SGK3 in HCC[34], and reverse chemoresistance of HCC cells by suppressing Nrf2[35]. In our work, EIF4G2 was found to be negatively regulated by miR-144, and the levels of miR-144 and EIF4G2 were reversely associated with each other in HCC samples. Consistent with other researches, we demonstrated that miR-144 suppressed HCC development in vitro and in vivo. Moreover, we discovered that re-expression of EIF4G2 could attenuate the inhibitory action of miR-144 on HCC.

Conclusion

Our discoveries first uncovered that EIF4G2 was increased in HCC tissues, and up-regulation of EIF4G2 was strongly associated with a poorer prognosis of HCC patients. In vitro and in vivo assays demonstrated that down-regulation of EIF4G2 could inhibit HCC cells growth, metastasis and HCC tumorigenesis through suppression the ERK signaling pathway. Finally, we found that miR-144 as a tumor suppressor, could negatively regulate EIF4G2 expression. Our findings revealed that EIF4G2 might be a promising therapeutic target in HCC and deserved more further studies in the future.

Abbreviations

HCC: Hepatocellular carcinoma; TMAs: tissue microarrays; IHC: Immunohistochemistry; miRNAs: MicroRNAs; TACE: transcatheter arterial chemoembolization; eIFs: eukaryotic translation initiation factors; EIF4G2: Eukaryotic translation initiation factor 4 gamma 2; Huh7-Luc: Huh7 cells stably expressing luciferase; RTCA: Real-Time Cell Analysis; RT-qPCR: Quantitative real-time polymerase chain reaction WT: wild-type; MUT: mutant; OS: overall survival; DFS: disease-free survival.

Additional File

Additional file 1:

Figure S1: Supplementary data.

Table S1: Clinical HCC patients' information.

Table S2: Sequences of primers.

Table S3: Sequences of siRNAs.

Declarations

Ethics approval and consent to participate

This research was allowed by the Medical Ethics Committee of the First Affiliated Hospital of Zhejiang University. All protocols of animal experiments were approved by the Animal Experimental Ethics

Committee of the First Affiliated Hospital of Zhejiang University.

Consent for publication

Not applicable.

Availability of data and materials

All data generated or analyzed during this study are included in this published article (and its supplementary information files).

Competing interests

The authors declare that they have no competing interests.

Funding

This study was sponsored by the State S & T Project of 13th Five Year (No. 2018ZX10302206), the National Natural Science Foundation of China (No. 81871646) and the Key R & D Projects of Zhejiang Province (2018C03019).

Authors' contributions

S.S.L collected clinical HCC samples and conducted the experiments. J.J.S and G.H.L helped build animal models. C.W did the work of Bioinformatics analysis. S.S.L, Y.N.L and M.Z designed the experiments. S.S.J and Y.N.L wrote the paper. All authors read and approved the final manuscript.

Acknowledgements

Not applicable.

References

1. Siegel RL, Miller KD, Jemal A. Cancer statistics. 2018. CA Cancer J Clin. 2018;68(1):7–30.
2. Bruix J, Reig M, Sherman M. Evidence-Based Diagnosis, Staging, and Treatment of Patients With Hepatocellular Carcinoma. Gastroenterology. 2016;150(4):835–53.
3. Bhat M, Robichaud N, Hulea L, Sonenberg N, Pelletier J, Topisirovic I. Targeting the translation machinery in cancer. Nat Rev Drug Discov. 2015;14(4):261–78.
4. Gantenbein N, Bernhart E, Anders I, Golob-Schwarzl N, Krassnig S, Wodlej C, et al. Influence of eukaryotic translation initiation factor 6 on non-small cell lung cancer development and progression. Eur J Cancer. 2018;101:165–80.
5. Golob-Schwarzl N, Krassnig S, Toeglhofer AM, Park YN, Gogg-Kamerer M, Vierlinger K, et al. New liver cancer biomarkers: PI3K/AKT/mTOR pathway members and eukaryotic translation initiation factors.

Eur J Cancer. 2017;83:56–70.

6. Lewis SM, Cerquozzi S, Graber TE, Ungureanu NH, Andrews M, Holcik M. The eIF4G homolog DAP5/p97 supports the translation of select mRNAs during endoplasmic reticulum stress. Nucleic Acids Res. 2007;36(1):168–78.
7. Warnakulasuriyarachchi D, Cerquozzi S, Cheung HH, Holcik M. Translational induction of the inhibitor of apoptosis protein HIAP2 during endoplasmic reticulum stress attenuates cell death and is mediated via an inducible internal ribosome entry site element. J Biol Chem. 2004;279(17):17148–57.
8. Nousch M, Reed V, Bryson-Richardson RJ, Currie PD, Preiss T. The eIF4G-homolog p97 can activate translation independent of caspase cleavage. RNA. 2007;13(3):374–84.
9. Emmrich S, Engeland F, El-Khatib M, Henke K, Obulkasim A, Schoning J, et al. miR-139-5p controls translation in myeloid leukemia through EIF4G2. Oncogene. 2016;35(14):1822–31.
10. Mazan-Mamczarz K, Zhao XF, Dai B, Steinhardt JJ, Peroutka RJ, Berk KL, et al. Down-regulation of eIF4GII by miR-520c-3p represses diffuse large B cell lymphoma development. PLoS Genet. 2014;10(1):e1004105.
11. Xie X, Li YS, Xiao WF, Deng ZH, He HB, Liu Q, et al. MicroRNA-379 inhibits the proliferation, migration and invasion of human osteosarcoma cells by targetting EIF4G2. Biosci Rep. 2017;37(3).
12. The Human Protein Atlas. https://www.proteinatlas.org/ENSG00000110321-EIF4G2/pathology/liver+cancer - Intensity. Accessed 15 March 2019.
13. GEPIA. http://gepia.cancer-pku.cn/detail.php?gene=EIF4G2. Accessed 15 March 2019.
14. Bartel DP. MicroRNAs: target recognition and regulatory functions. Cell. 2009;136(2):215–33.
15. Lou G, Chen L, Xia C, Wang W, Qi J, Li A, et al. MiR-199a-modified exosomes from adipose tissue-derived mesenchymal stem cells improve hepatocellular carcinoma chemosensitivity through mTOR pathway. Journal of Experimental & Clinical Cancer Research. 2020;39(1).
16. Liu Y, Lou G, Norton JT, Wang C, Kandela I, Tang S, et al. 6-Methoxyethylamino-numonafide inhibits hepatocellular carcinoma xenograft growth as a single agent and in combination with sorafenib. FASEB J. 2017;31(12):5453–65.
17. Liu Y, Zhang X, Yang B, Zhuang H, Guo H, Wei W, et al. Demethylation-Induced Overexpression of Shc3 Drives c-Raf-Independent Activation of MEK/ERK in HCC. Cancer Res. 2018;78(9):2219–32.
18. Ito Y, Sasaki Y, Horimoto M, Wada S, Tanaka Y, Kasahara A, et al. Activation of mitogen-activated protein kinases/extracellular signal-regulated kinases in human hepatocellular carcinoma. Hepatology. 1998;27(4):951–8.
19. Lan F, Yu H, Hu M, Xia T, Yue X. miR-144-3p exerts anti-tumor effects in glioblastoma by targeting c-Met. J Neurochem. 2015;135(2):274–86.
20. Jahanbani I, Al-Abdallah A, Ali RH, Al-Brahim N, Mojiminiyi O. Discriminatory miRNAs for the Management of Papillary Thyroid Carcinoma and Noninvasive Follicular Thyroid Neoplasms with Papillary-Like Nuclear Features. Thyroid. 2018;28(3):319–27.

21. Wang H, Wang A, Hu Z, Xu X, Liu Z, Wang Z. A Critical Role of miR-144 in Diffuse Large B-cell Lymphoma Proliferation and Invasion. Cancer Immunol Res. 2016;4(4):337–44.
22. Nakagawa S, Wei L, Song WM, Higashi T, Ghoshal S, Kim RS, et al. Molecular Liver Cancer Prevention in Cirrhosis by Organ Transcriptome Analysis and Lysophosphatidic Acid Pathway Inhibition. Cancer Cell. 2016;30(6):879–90.
23. Goossens N, Sun X, Hoshida Y. Molecular classification of hepatocellular carcinoma: potential therapeutic implications. Hepat Oncol. 2015;2(4):371–9.
24. Weingarten-Gabbay S, Khan D, Liberman N, Yoffe Y, Bialik S, Das S, et al. The translation initiation factor DAP5 promotes IRES-driven translation of p53 mRNA. Oncogene. 2014;33(5):611–8.
25. de la Parra C, Ernlund A, Alard A, Ruggles K, Ueberheide B, Schneider RJ. A widespread alternate form of cap-dependent mRNA translation initiation. Nat Commun. 2018;9(1):3068.
26. Bellsolell L, Cho-Park PF, Poulin F, Sonenberg N, Burley SK. Two structurally atypical HEAT domains in the C-terminal portion of human eIF4G support binding to eIF4A and Mnk1. Structure. 2006;14(5):913–23.
27. Marash L, Liberman N, Henis-Korenblit S, Sivan G, Reem E, Elroy-Stein O, et al. DAP5 promotes cap-independent translation of Bcl-2 and CDK1 to facilitate cell survival during mitosis. Mol Cell. 2008;30(4):447–59.
28. Hundsdoerfer P, Thoma C, Hentze MW. Eukaryotic translation initiation factor 4GI and p97 promote cellular internal ribosome entry sequence-driven translation. Proc Natl Acad Sci U S A. 2005;102(38):13421–6.
29. Zhao H, Wang A, Zhang Z. LncRNA SDHAP1 confers paclitaxel resistance of ovarian cancer by regulating EIF4G2 expression via miR-4465. J Biochem. 2020.
30. Hao GJ, Hao HJ, Ding YH, Wen H, Li XF, Wang QR, et al. Suppression of EIF4G2 by miR-379 potentiates the cisplatin chemosensitivity in nonsmall cell lung cancer cells. FEBS Lett. 2017;591(4):636–45.
31. Sugiyama H, Takahashi K, Yamamoto T, Iwasaki M, Narita M, Nakamura M, et al. Nat1 promotes translation of specific proteins that induce differentiation of mouse embryonic stem cells. Proc Natl Acad Sci U S A. 2017;114(2):340–5.
32. Liang HW, Ye ZH, Yin SY, Mo WJ, Wang HL, Zhao JC, et al. A comprehensive insight into the clinicopathologic significance of miR-144-3p in hepatocellular carcinoma. Onco Targets Ther. 2017;10:3405–19.
33. Gu J, Liu X, Li J, He Y. MicroRNA-144 inhibits cell proliferation, migration and invasion in human hepatocellular carcinoma by targeting CCNB1. Cancer Cell Int. 2019;19:15.
34. Wu M, Huang C, Huang X, Liang R, Feng Y, Luo X. MicroRNA-144-3p suppresses tumor growth and angiogenesis by targeting SGK3 in hepatocellular carcinoma. Oncol Rep. 2017;38(4):2173–81.
35. Zhou S, Ye W, Zhang Y, Yu D, Shao Q, Liang J, et al. miR-144 reverses chemoresistance of hepatocellular carcinoma cell lines by targeting Nrf2-dependent antioxidant pathway. Am J Transl Res. 2016;8(7):2992–3002.

Table

Table 1 Correlation between EIF4G2 expression and clinicopathological characteristics

	Variables	EIF4G2 expression		χ2	p-value
		high	low		
Age (year)				4.066	0.044
	≤50	24	15		
	＞50	20	30		
Sex				0.001	0.970
	Female	5	5		
	Male	39	40		
Grade				3.236	0.072
	1/2	25	17		
	3	19	28		
T stage				6.612	**0.010**
	T1	34	23		
	T2/T3	10	22		
TNM stage				6.612	**0.010**
	I	34	23		
	II/III	10	22		
PDL1				4.443	**0.035**
	Negative	30	20		
	Positive	12	21		
Recurrence				4.048	**0.044**
	No	25	16		
	Yes	19	29		

Note: Bold p values display statistical significance, P<0.05.

Figures

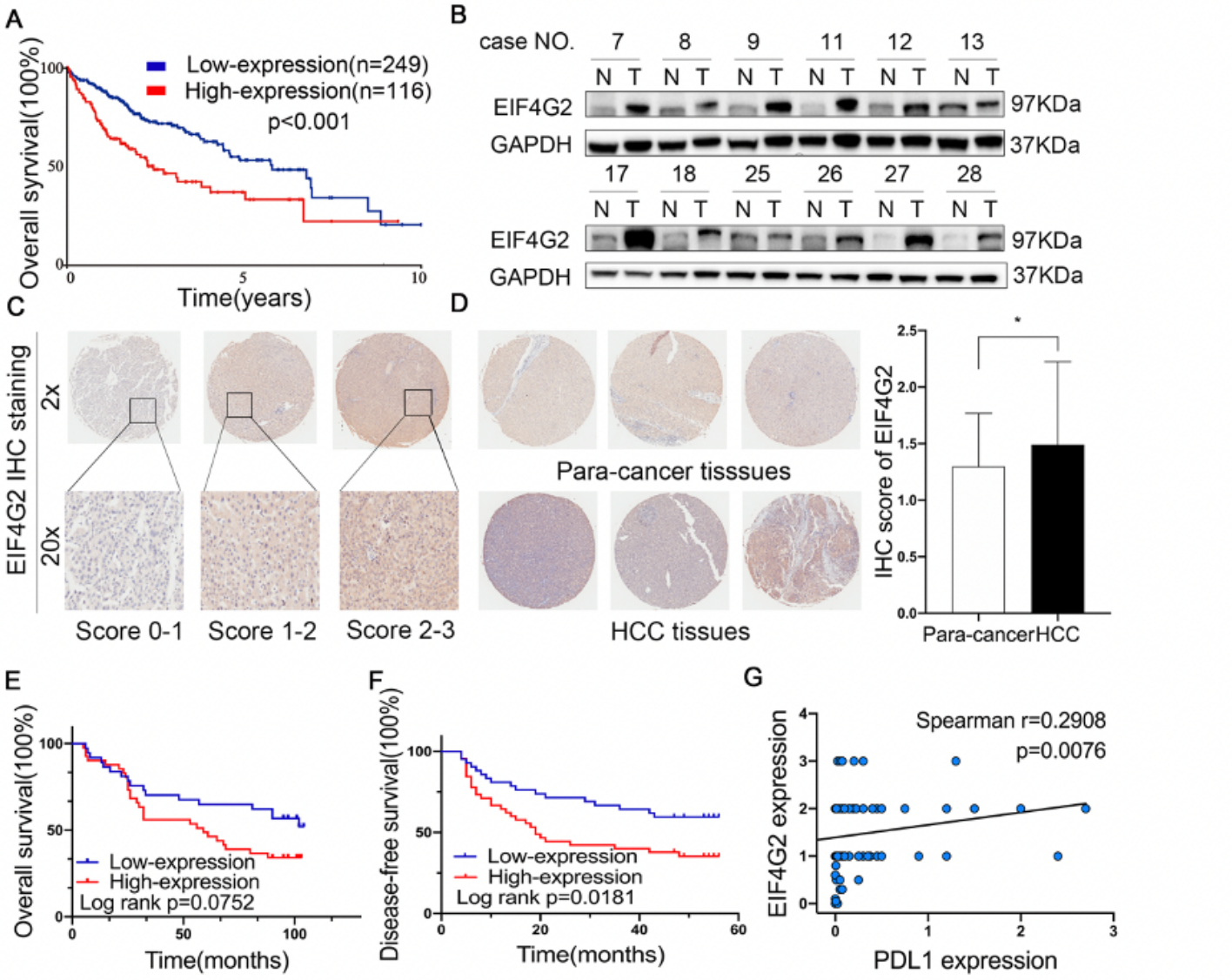

Figure 1

EIF4G2 is overexpressed in HCC and high EIF4G2 expression indicates poor prognosis of HCC patients. (A) OS analysis in HCC patients with high- or low-expression of EIF4G2 from the Human Protein Atlas database. (B) Representative images of EIF4G2 expression in 30 paired HCC tissues(T) and adjacent para-carcinoma tissues(N). (C) Representative images of EIF4G2 IHC staining with different staining scores. Images were presented at 2x magnification (up panel) and 20x magnification (lower panel). (D) Representative images and analysis of EIF4G2 IHC staining in HCC tissues and adjacent para-carcinoma tissues, images were presented at 2x magnification. (E) Kaplan–Meier curves analysis of OS in HCC-TMA patients with high- or low-expression of EIF4G2. (F) Kaplan–Meier curves demonstrating DFS in HCC-TMA patients with high- or low-expression of EIF4G2. (G) Spearman's correlation analysis of EIF4G2 expression and PDL1 expression. *p < 0.05.

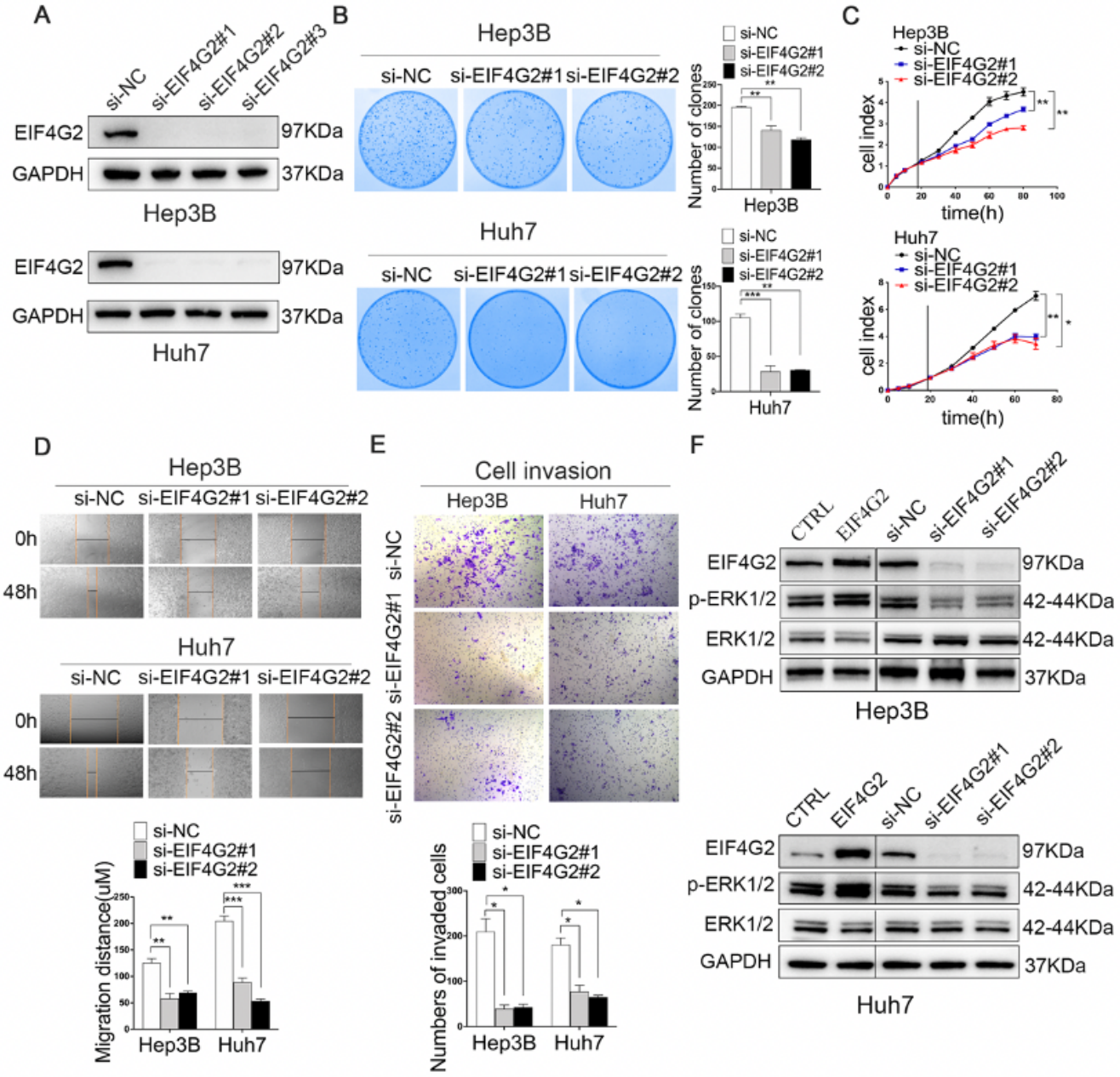

Figure 2

EIF4G2 facilitates HCC growth and metastasis in vitro. (A) HCC cells Hep3B and Huh7 cells were transfected with negative control (NC) or three different si-RNAs of EIF4G2. The knockdown efficiency of EIF4G2 was measured by Western blot. (B) Functions of EIF4G2 knockdown on HCC cells proliferation were performed by colony formation assay. (C) RTCA analysis of cells proliferation in Hep3B and Huh7 cells. (D) Functions of EIF4G2 knockdown on HCC cells migration were determined by scratch experiment. (E) Effects of EIF4G2 knockdown on HCC cells invasion were detected by transwell invasion assays. (F) Two HCC cells were transfected with NC, si-EIF4G2 or EIF4G2 overexpress vector, and the level of ERK1/2 and p-ERK1/2 was determined by Western blot. *p < 0.05, **p < 0.01, ***p < 0.001.

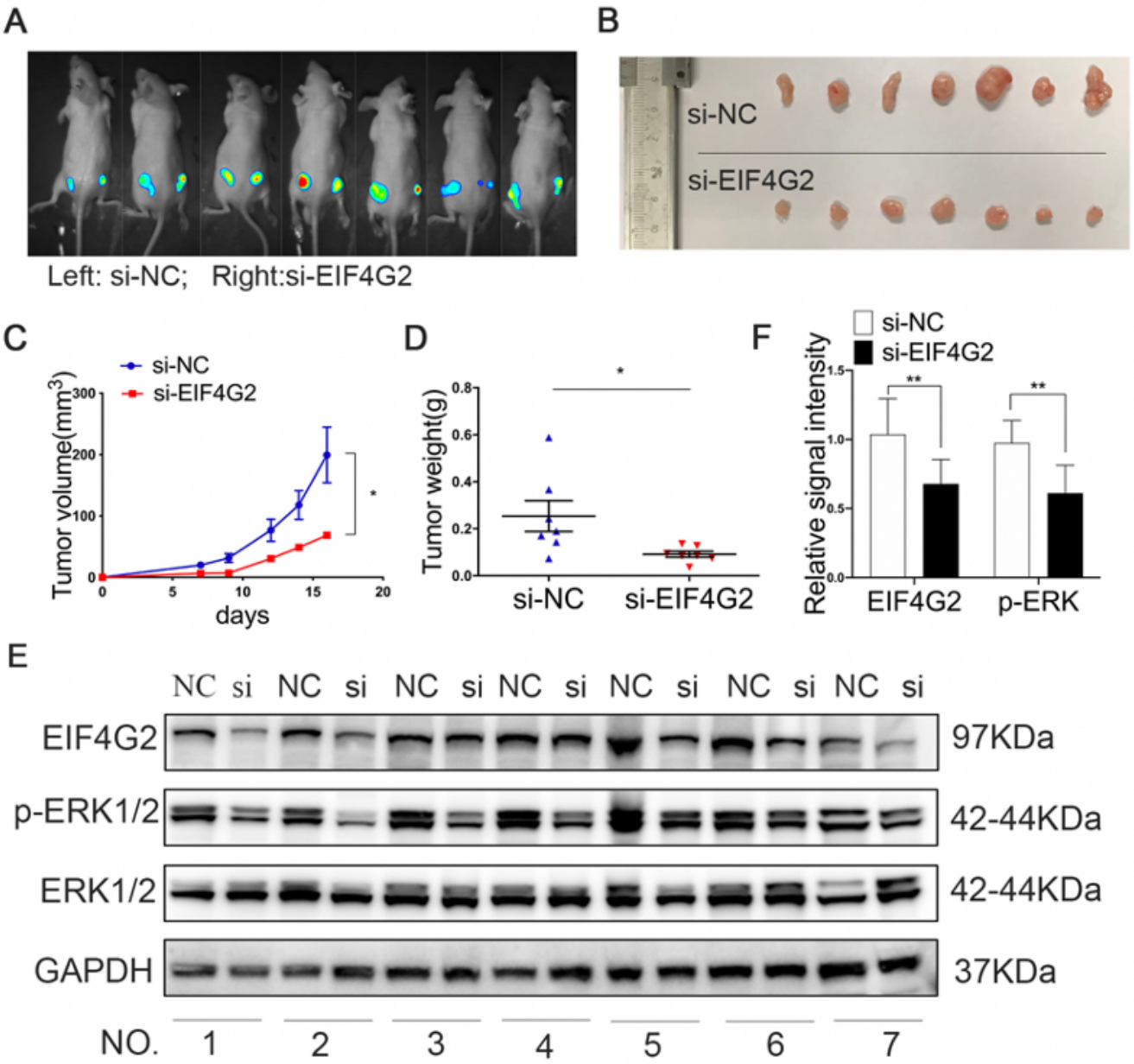

Figure 3

EIF4G2 knockdown suppresses tumorigenesis in vivo. (A) Fluorescent photos of nude mice bearing HCC tumors. (B) Representative of HCC tumors from NC and si-EIF4G2 groups. (C) The tumor growth curves. (D) HCC tumor weight was measured, and the results were presented as mean ± S.D. (E) The expression of EIF4G2, ERK1/2 and p-ERK1/2 proteins in mice tumor were measured with Western blot. (F) Relative signal intensity of EIF4G2 and p-ERK1/2 proteins level of WB. *p < 0.05, ** p < 0.01.

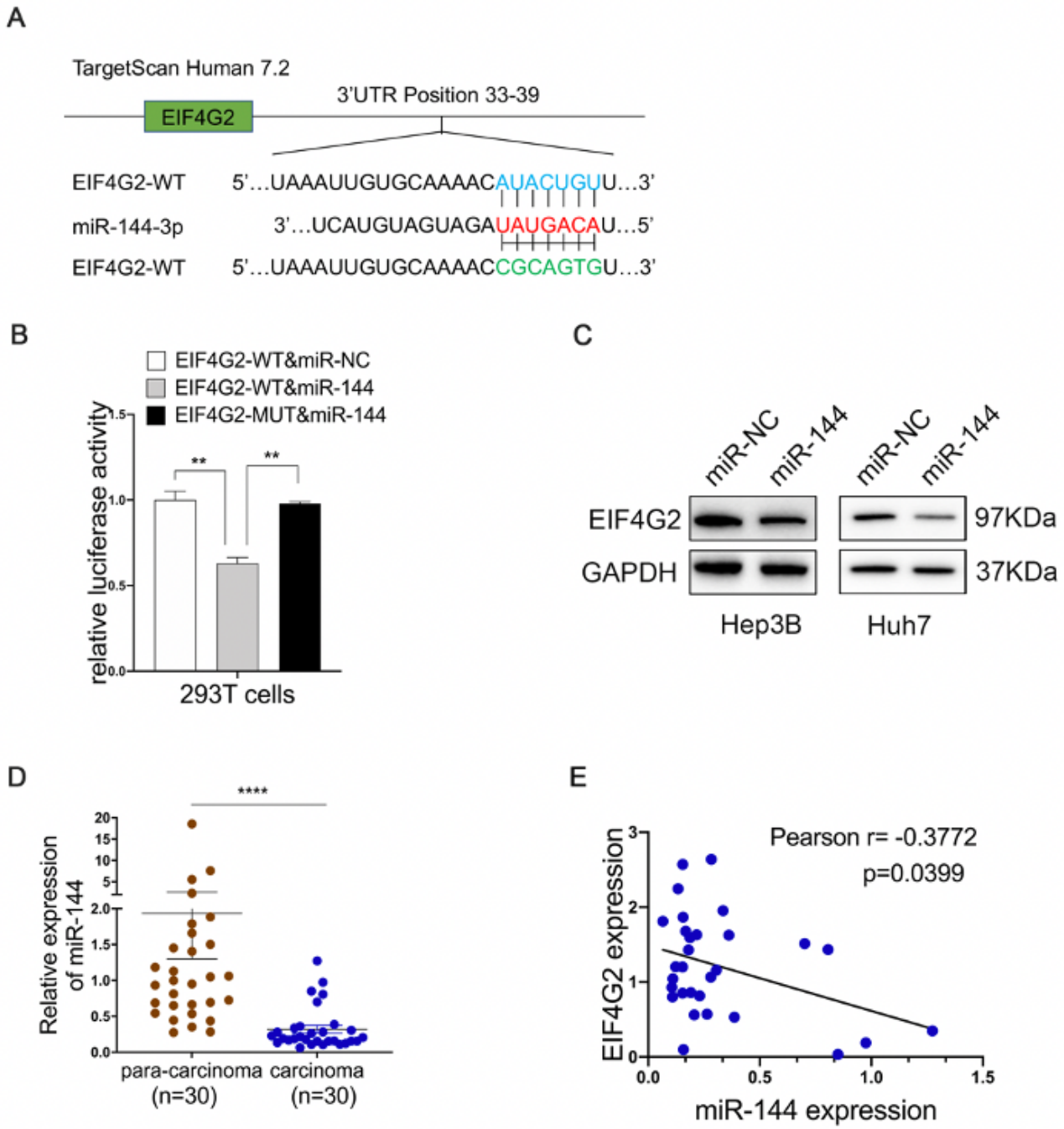

Figure 4

EIF4G2 is negatively regulated by miR-144. (A) Putative binding sites between miR-144 and EIF4G2-WT or EIF4G2-MUT 3'UTR position. (B) Luciferase reporter vectors of EIF4G2-WT or EIF4G2-MUT and miR-144 overexpression vectors were co-transfected into 293T cells. Relative luciferase activity was assessed 48h later. (C) Western blot analysis of EIF4G2 level. (D) The expression of miR-144 in HCC tumor tissues and matched para-cancer tissues. (E) Pearson association analysis of the miR-144 level and EIF4G2 protein expression. **p < 0.01, ****p < 0.0001 WT: the wild-type vector, MUT: the mutant vector.

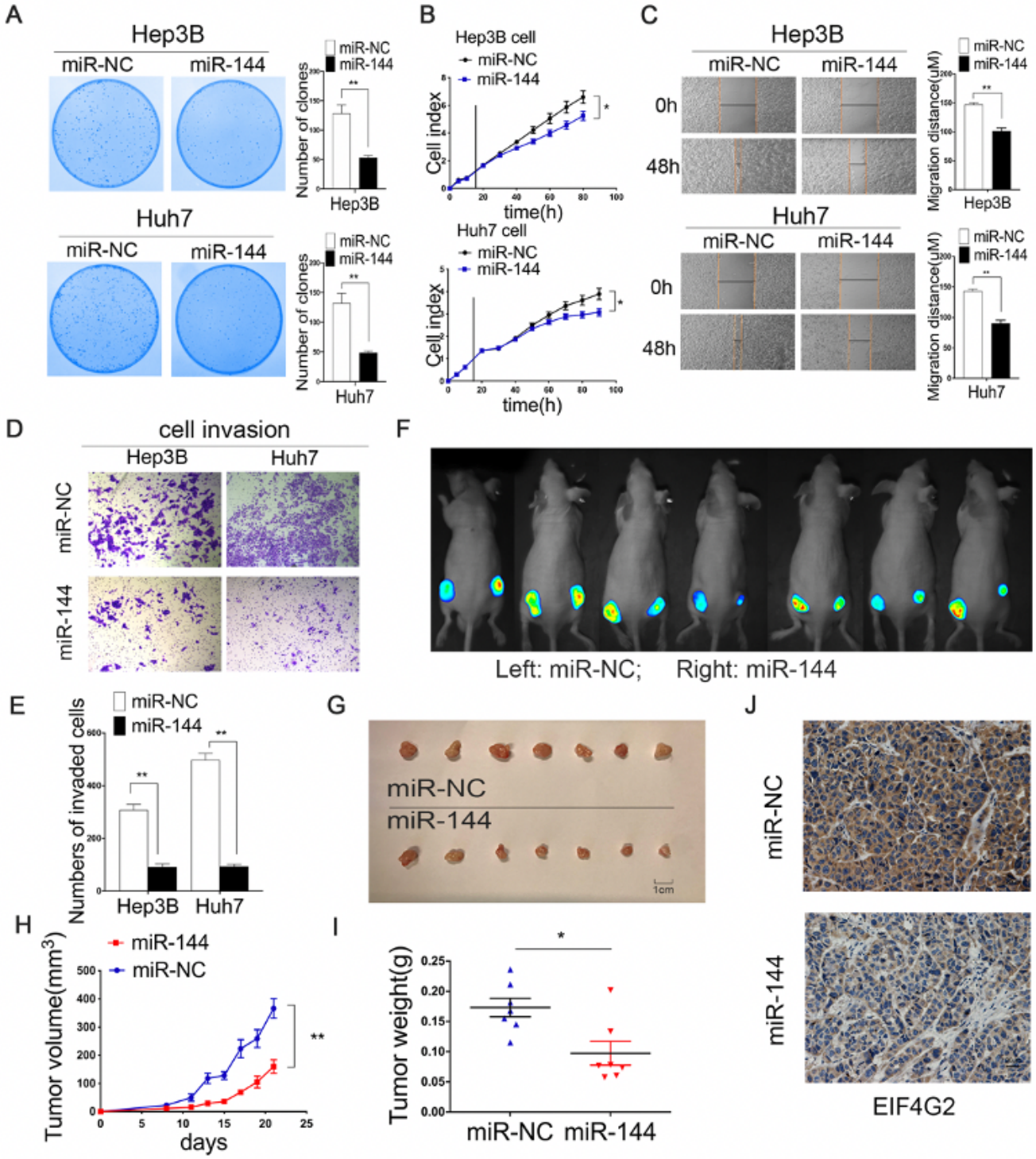

Figure 5

MiR-144 suppresses HCC development in vitro and in vivo. (A) Functions of overexpression of miR-144 on Hep3B and Huh7 cells were determined by colony formation assay. (B) RTCA analysis of cells proliferation in two HCC cells (The vertical line represented the time of cell transfection). (C) Cells migration ability was assessed by wound healing assay. (D) Cells invasion ability was measured by transwell invasion assay. (E) Statistical analysis of the invaded cells. (F) Fluorescent photos of nude

mice bearing HCC tumors. (G) Representative of HCC tumors from NC and miR-144 overexpression groups. (H) The tumor growth curves. (I) HCC tumor weight was measured. (J) Representative images of EIF4G2 IHC staining of mice tumor sections from NC and miR-144 group. * p < 0.05, **p < 0.01

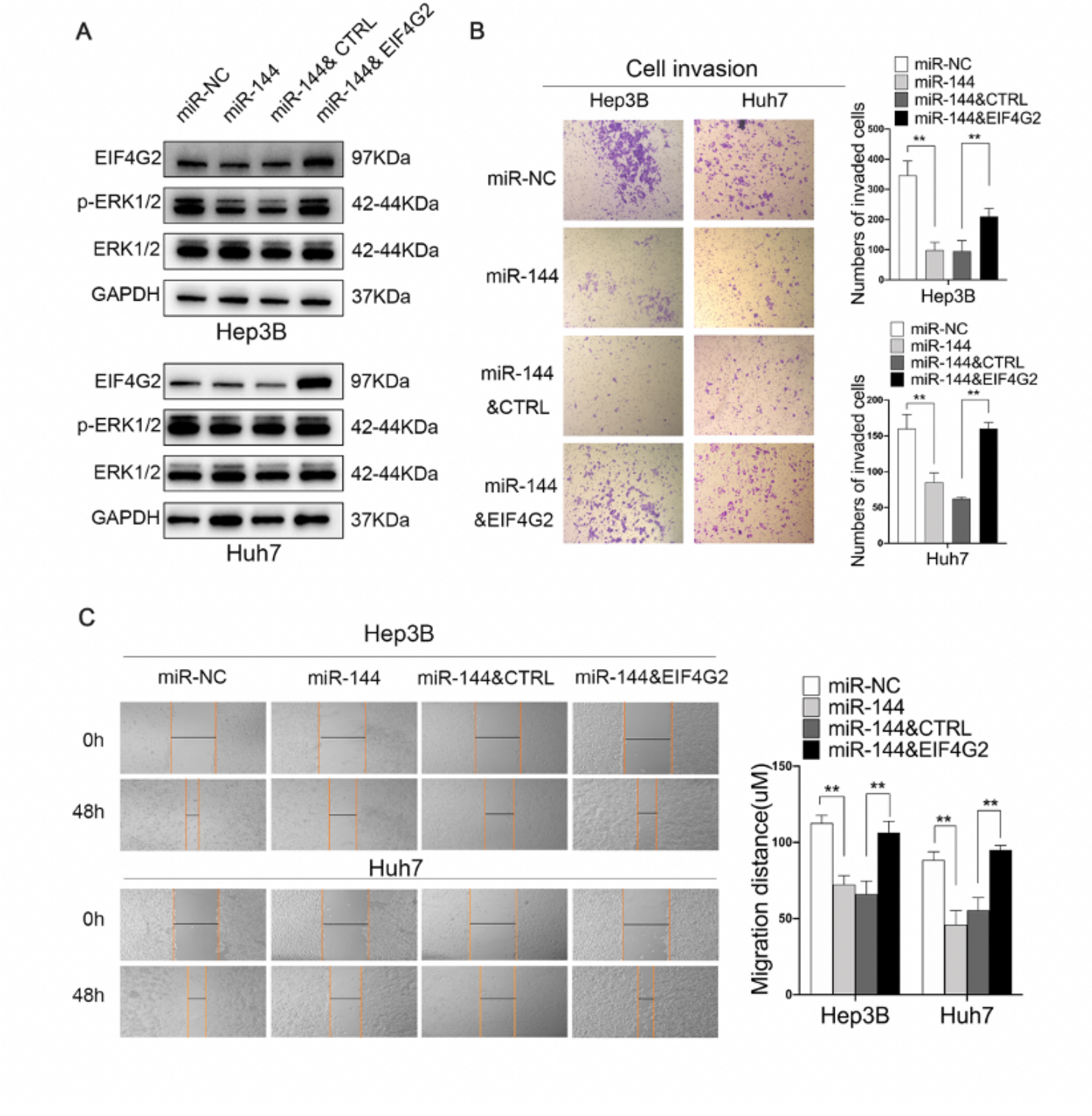

Figure 6

Functions of EIF4G2 in HCC are regulated by miR-144. (A) Western blot analysis of EIF4G2, ERK1/2 and p-ERK1/2 expression. (B) The migration ability was performed with scratch experiments. (C) The invasion ability was assessed by transwell invasion assays. **p < 0.01.

Supplementary Files

This is a list of supplementary files associated with this preprint. Click to download.

- Supplementarydata.docx